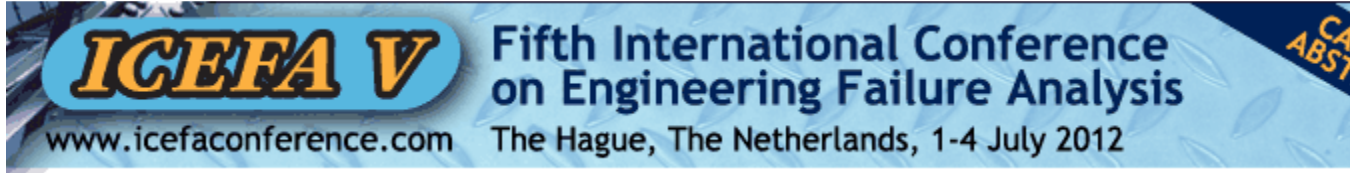




Articles All fields Author
 Images Journal/Book title Volume Issue Page



[PDF \(967 K\)](#) [Export citation](#) [E-mail article](#)

Article [Figures/Tables \(19\)](#) [References \(19\)](#) [Thumbnails](#) | [Full-Size images](#)

Engineering Failure Analysis
 Volume 18, Issue 1, January 2011, Pages 421-432

doi:10.1016/j.engfailanal.2010.09.030 | [How to Cite or Link Using DOI](#)
[Permissions & Reprints](#)

Time-dependent reliability analysis of B70 pre-stressed concrete sleeper subject to deterioration

[Saeed Mohammadzadeh](#) , [Ehsan Vahabi](#)

School of Railway Engineering, Iran University of Science and Technology, Iran

Received 27 June 2010; revised 28 September 2010; Accepted 28 September 2010. Available online 10 October 2010.

Abstract

Railway sleepers are amongst the vital components of the rail track superstructure and play significant role in providing integrity and safe operation of the tracks. Such sleepers are manufactured with different composition among them pre-stressed concrete sleepers are more common. From the durability and the track resistance point of view, the sleepers that originate from the same factory possess almost the same mechanical properties. However, they may end up in different working conditions. Similar to all other types of structures, an initial reliability index can be assigned to pre-stressed concrete sleepers in the beginning of their service life. Naturally, this index decreases over the time according to the environmental conditions. The authors of this article have investigated the impact of penetration of chloride ion on reliability index of

Rela

- [Relia](#)
- [Com](#)
- [Relia](#)
- [Com](#)
- [Prob](#)
- [Engir](#)
- [PERT](#)
- [probe](#)
- [Struc](#)
- [Relia](#)
- [Struc](#)

[View](#)

My Ap

[Add](#)



Find
dow

[Abou](#)

B70 pre-stressed concrete sleeper. It is the purpose of this paper to present the correlation between the corrosion due to chloride ion and the reliability index of the concrete sleepers. UIC713 code is used to provide for the loading conditions and the analysis of concrete sleepers. The limit state function that is used for the pre-stressed concrete reliability analysis is based on the allowable stress criteria. The simulation procedures that are used in this article are based on a computational reliability model and the Monte Carlo technique. The change in the reliability index is calculated in points with significant tensile stresses, such as the top fiber of the sleeper, the mid-span and the bottom fiber of the rail seat. The sensitivity analyses indicate that the sleeper reliability is considerably sensitive to the variations of dimension, the strength and the loading of the sleeper. It is concluded that the sleeper mid-span is more vulnerable than the rail seat and the failure at this point is more likely to occur.

Keywords: Time-dependent reliability; Pre-stressed concrete sleeper; Corrosion; Chloride diffusion

Article Outline

1. [Introduction](#)
2. [Problem definition](#)
 - 2.1. [Safety level](#)
 - 2.2. [Methodology](#)
3. [The design and analysis of pre-stressed concrete sleeper](#)
 - 3.1. [Analysis of the forces acting on the sleeper](#)
 - 3.2. [Stress in the pre-stressed concrete sleeper](#)
4. [Probabilistic model of corrosion](#)
 - 4.1. [The chloride diffusion models](#)
 - 4.2. [The corrosion rate model](#)
 - 4.3. [Reduction of the cross-sectional area of the sleeper bars](#)
5. [Time dependent analysis of the reliability](#)
 - 5.1. [Probabilistic model of the load and the strength](#)
 - 5.2. [The analysis of the reliability in operation](#)
 - 5.3. [Variation of the reliability with respect to time](#)
 - 5.4. [The Sensitivity analysis of reliability variations](#)

6. [Conclusion](#)

[References](#)

1. [Introduction](#)

Railway sleepers are amongst the important railway superstructures that lie between the rail and the ballast. Sleepers are composed of several materials. The most common type of the sleepers are made of the pre-stressed concrete [1]. Determination of the health and the performance of the sleepers is a key factor in maintaining railways [2]. Performance of the pre-stressed concrete sleeper is the same as a pre-cast beam in withstanding the rail forces and the compression stresses exerted by the underlying ballast layer. [Fig. 1](#) shows a typical railway track.



Cite

- [This](#)

Rela

- [Com](#)
- [Ency](#)
- [Mont](#)
- [Interr](#)
- [1.03](#)
- [Com](#)
- [Mark](#)
- [Interr](#)
- [2.13](#)
- [Treat](#)

▶ [More](#)

[View F](#)



Resear
differe





Over the past two decades, durability and longevity of concrete structures have been the focus of many researches [3]. There are several good reasons for such interests. The environmental conditions that cause deterioration and corrosion in concrete structures are amongst them. The time and the intensity of the failure are dependent on the type of concrete and the environmental conditions. One of the significant factors that causes the sleeper deterioration and leads to lifetime reduction is the corrosion of the bars under the influence of chloride ion.

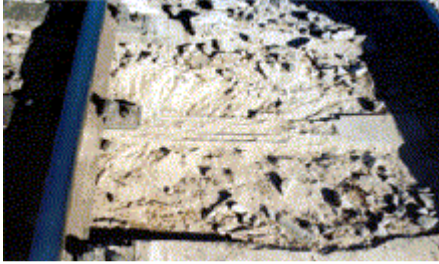
In the sleeper design and construction processes, attention is paid to the nominal resistance, while durability and lifetime are usually neglected. This happens while the sleeper is expected to perform in near destructive environmental conditions. The working zones for using the sleepers in individual countries are as wide as the railway network in such countries. The pre-stressed concrete sleepers like other structures have specific reliability index and probability of failure.

One of the most recent methods for obtaining the failure probability of structures is based on the reliability theory. In this design approach, a specific reliability is determined for the concrete structure. Although, assessment of reliability indicates safety of the structure in early stages of the operation, but it does not determine failure probability of the structure during service. As demonstrated in [4] and [5], the reliability of pre-stressed concrete sleepers has been evaluated in Iran and Australia during the initial stages of the operation. This main objective of this research is to report variations in the reliability of the type B70 sleepers in conjunction with the corrosion of bars during its operation period. It needs to be noted that corrosion of the bars is one of the main reasons for replacing sleepers in harsh and destructive environments. Several methods for the analyses of the internal sleeper forces are discussed that are based on the design codes. In this article, loading and the analysis of the railway sleeper is based on the instructions that are provided in the UIC713 code. All the influential parameters in the reliability analysis and the limit state function are considered as uncertain parameters.

2. Problem definition

In order to investigate the sleeper deterioration, the environmental factors that are effective in the deterioration need to be investigated, first. In order to increase the durability of concrete in sleeper production, low water to cement ratios are used [4]. In Iran, for pre-stressed type B70 concrete sleeper the mandate for the water to cement ratio is 0.35. This assists in decreasing the penetration of ions into the sleeper concrete. For the purposes of this research, the probability and the time of sleeper failure are calculated based on some input data that are extracted from the field measurements.

The selected railway path is located in an environment with fine-graded soil and the relative humidity of about 30%. It is also possible for the local winds to spread soils over the sleepers. Moisture and rain provide a susceptible environment that causes corrosion of bars in the concrete. Low water to cement ratio makes the sleeper sufficiently resistant to other climatic conditions such as the temperature variations that has a minor effect on the deterioration of sleeper in this location [6]. Observations indicate that the main factor causing failure in the sleepers is corrosion of the bars that is due to the presence of the chloride ion. Fig. 2 indicates the sleeper destruction due to bar corrosion.



[Full-size image \(45K\)](#)

Fig. 2.

The railway sleeper destruction caused by the bar corrosion.

2.1. Safety level

In order to calculate the reliability of a structure, the limit state function, safety and performance level need to be initially defined. The limit state function is the boundary between the safety and the failure of the structure. Generally, in the limit state approach, the structural safety margin function can be defined by Eq. (1). [7].

$$g(x) = \text{Capacity} - \text{Demand} = R(x) - Q(x) \quad (1)$$

If $g(x) > 0$ the structure is safe. The probability of the failure can be obtained by using Eq. (2).

$$P_f = P[g(x) \leq 0] = \int \dots \int f(x)(x_1, \dots, x_n) dx_1 \dots dx_n \quad (2)$$

where $g(x)$ is a limit state function and $f(x)(x_1, \dots, x_n)$ is the probability density function of x random variables. There are several methods to investigate the reliability index. These methods include the first and the second order reliability methods (FORM and SORM) and the Monte Carlo simulation method. In this research, the initial reliability index is computed by using all of the three mentioned methods. Eventually, the procedures ended up to the identical results. The Monte Carlo simulation is utilized to obtain variation of the reliability during the lifetime of a structure.

2.2. Methodology

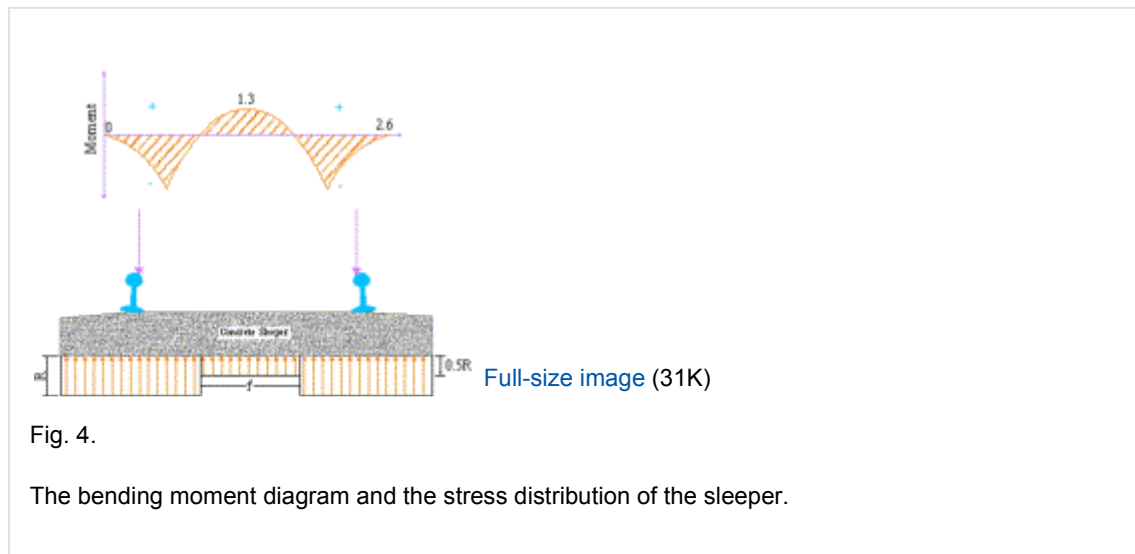
One of the main reasons for the decrease in the sleeper bending strength is the corrosion of internal bars in the presence of chloride ion. The methodology of this paper for the investigation of the impact of steel bars corrosion on the sleeper failure is based upon field and laboratory investigation of concrete samples along with the computational methods. The computational methods consist of the statistical analysis of the experimental results and the reliability evaluation under the corrosion conditions. The problem-solving methodology used in this paper is shown in Fig. 3.



3. The design and analysis of pre-stressed concrete sleeper

The design methods of the concrete pre-stress sleeper are similar to the pre-stressed concrete beam that is based on the allowable stress on the top and the bottom fibers of the beam.

The sleeper internal stresses are created by the influence of the rail forces and the compression stresses due to the ballast [8] and [9]. Due to some factors, such as the unequal qualities of ballast tamping and the different types of the ballast grading, the distribution of stress under the sleeper is not uniform. Fig. 4 indicates the stress distribution beneath the sleeper that is mentioned in UIC713 code.



3.1. Analysis of the forces acting on the sleeper

In order to calculate the sleeper internal stresses, the initial state is to determine the moments and the forces that are imposed by the rail on the sleeper. For the purposes of this research, the maximum axle load is 25 tonnes and the maximum train speed of travel is considered to be 120 km/h.

There are several standards for the calculation of the equivalent static wheel load such as the AREMA [8], UIC713 [9], and the Australian standards [5]. Eq. (3) presents the equivalent static wheel load based on the UIC713 code.

$$Qr=q/2(1+\gamma_p \times \gamma_v) \times \gamma_d \times \gamma_r = 117 \text{Kn}$$

where $\gamma_p = 0.75$ is the dynamic factor that is an indicator of the rail pad attenuation, $\gamma_v = 0.5$ is the speed factor, $\gamma_r = 1.35$ is the sleeper reaction factor that allows variation in the sleeper reaction and $\gamma_d = 0.5$ is the load distribution factor between the sleepers. In the UIC713 code the bending moment at the rail seat can be calculated using the following equation:

$$(M_r = \gamma_i \times Qr \times \gamma/2)$$

where γ_i is the dynamic amplification coefficient of the bending moment due to the irregularities in the longitudinal support of the sleeper and γ is the effective lever arm that is 0.183 m [9].

3.2. Stress in the pre-stressed concrete sleeper

The pre-stressed concert sleeper is designed according to the UIC713 regulations and based on the allowable stresses at the top and bottom fibers. Generally, these stresses can be defined by using Eqs. (4) and (5)[10].

$$f_t = -\frac{P}{A} + \frac{P \times e}{Z_t} - \frac{M}{Z_t} \tag{4}$$

$$f_b = -\frac{P}{A} + \frac{P \times e}{Z_b} - \frac{M}{Z_b} \tag{5}$$

where f_t and f_b are the allowable stresses at the top and bottom fibers, P is the pre-stressing force, e is the eccentricity, and M is the bending moment at the rail seat. Z_b and Z_t are the section modulus for the bottom and the top fibers and A is the cross-sectional area of the member. The rail seat and the mid-span section of the B70 Sleeper are illustrated in Fig. 5[4]. The average strength of the cylindrical specimens of the concrete sleeper is 55 MPa. The Bending moment and the stresses at the rail seat and mid-span are presented in Table 1.

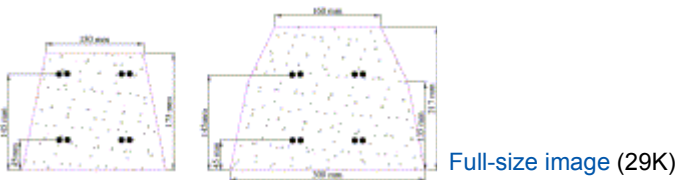


Fig. 5.

The mid-span (Left) and the rail seat (Right) sections of the B70 Sleeper.

Table 1. Bending moment and stresses at rail seat and mid-span.

	Moment (KN-m)	Position	Allowable stress (MPa)	Total stress (MPa)
Rail Seat	17.2KN-m	Top fiber	-24.75	-15.94
		Bottom fiber	3.71	1.54
		Top fiber	3.71	3.04

Moment (KN-m)	Position	Allowable stress (MPa)	Total stress (MPa)
	Bottom fiber	-24.75	-22.66

4. Probabilistic model of corrosion

Corrosion can have severe implications on the lifetime of the concrete structures [11]. Corrosion is the most influential factor in reducing the cross-section of the steel bars. The chloride diffusion rate depends on different factors including the concrete cover. In the following section of this article, simulation models of chloride ion penetration are presented [6] and [3].

4.1. The chloride diffusion models

The process of the chloride ingress into the concrete is generally based on the Fick’s second law of diffusion [12]. Eq. (6) illustrates the second Fick’s law by a partial differential equation. Initial amount of the chloride ion is usually less than 1%. For the purposes of this research, the initial chloride ion content is assumed to be zero.

$$\frac{dC(x, t)}{dt} = D_c \frac{d^2 C(x, t)}{dx^2} \tag{6}$$

where x is the concrete cover (cm), C is the chloride concentration at x , D_c is the chloride diffusion coefficient (cm^2/year) and t is the time (s). Solving the differential Eq. (6) leads to the following equation:

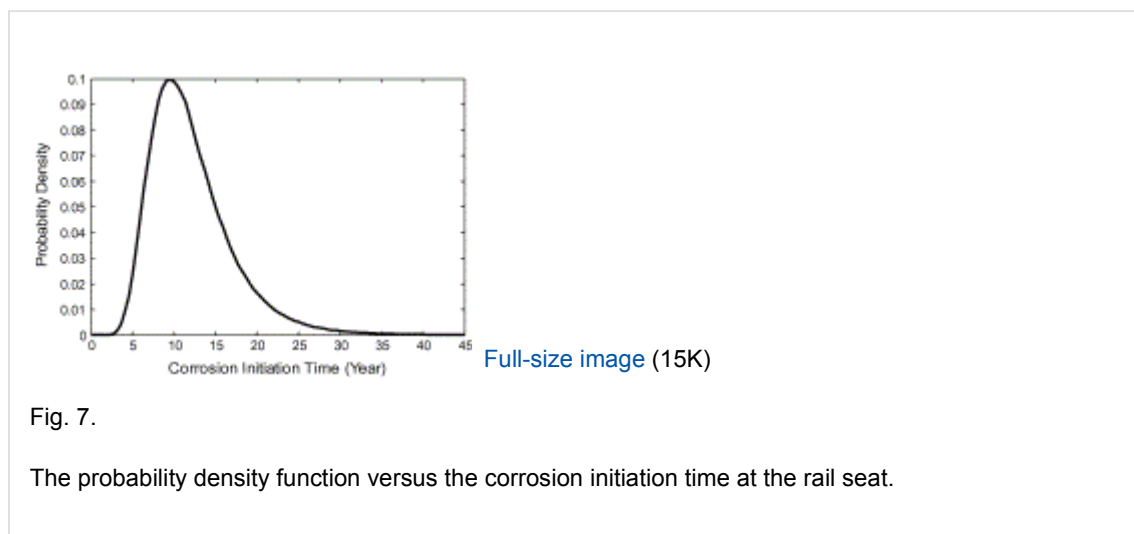
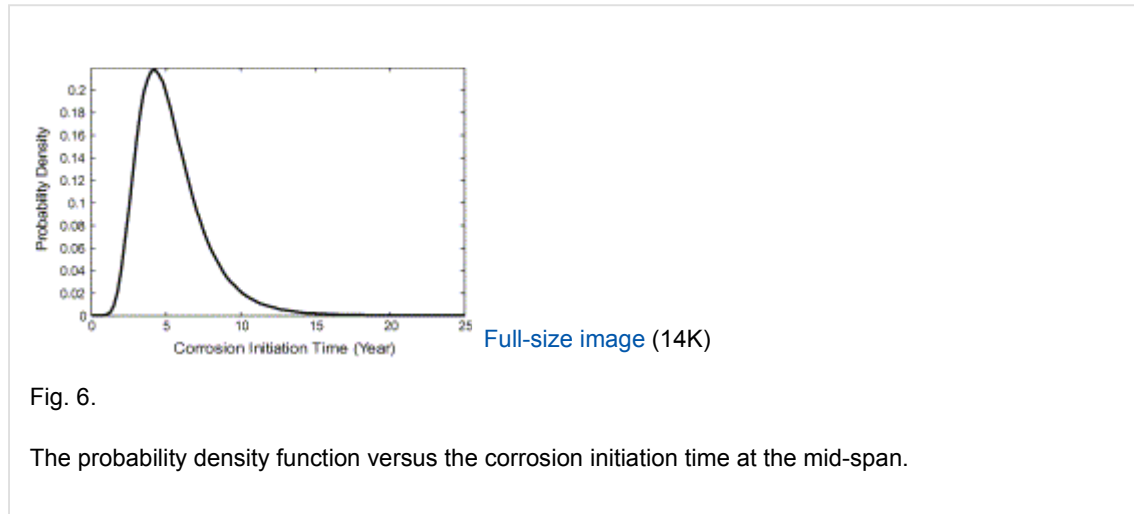
$$C(x, t) = C_s \left(1 - \text{erf} \frac{x}{2 \sqrt{D_c t}} \right) \tag{7}$$

where C_s is the chloride concentration at the concrete surface (% weight of concrete). erf is the statistical error function. The chloride diffusion coefficient depends on the concrete properties such as the water–cement ratio and the material–cement ratio as well as the environmental conditions such as the temperature and humidity. It should be noted that the parameters D_c , C_s and x are uncertain parameters and consequently $C(x,t)$ is also an uncertain parameter. If the chloride concentration around the bar surface reaches to its critical level then in order to predict the time of initial corrosion, Eq. (7) need to be rearranged for the time variable and the chloride critical concentration C_{cr} , at a given effective depth x [3]. Using the Monte Carlo simulation, and considering the type of distribution of the statistical parameters shown in Table 2[13] and [4] the time of the initial corrosion can be calculated [14].

Table 2. Statistical properties of corrosion parameters.

Variable	average	Variation coefficient	Type of distribution	Ref.
C_s	0.381	0.20	Normal	[6]
C_{cr}	0.06	0.12	Normal	[6]
$D_c(\text{cm}^2/\text{year})$	0.48	0.3	Lognormal	[6]
$x = 3 \text{ cm}$	3 cm	0.1	Normal	[18]
T (year)			Normal	

Fig. 6 shows the probability density function of the initial corrosion in the sleeper mid-span that is obtained after generation of 10,00,000 random numbers. The computer program that is tailored for the calculation of the Monte Carlo numbers is based on the commercially available software program, MATLAB version 2008a. The best fit for the probability density function is lognormal and it is predicted that the time of the corrosion initiation of the sleeper mid-span is 5.5 year. In the rail seat, however, according to the results that are presented in Fig. 7, and considering the increase of the concrete cover to 45 mm, the initial deterioration time has increased to 12 years.



4.2. The corrosion rate model

When the amount of the chloride ions around the sleeper bars reaches to a specific level, assuming that all of the other conditions are provided, corrosion begins in the bars with failure of the passive film. This leads to a decrease in the bar cross-sectional area. The corrosion rate can be restrained by controlling the amount of the water and oxygen at the steel surface [13] and [15]. In other words, when the protective oxide layer on the bar breaks, the corrosion rate depends on the amount of the moisture and oxygen in the vicinity of the bars. Stewart expressed an empirical formula for the annual corrosion rate that depends on the water to cement ratio and the concrete cover [16]. Eq. (8) depicts this empirical formula:

$$i_{corr}(1) = \frac{37.8(1 - \frac{w}{c})^{1.84}}{cover}$$

where w/c is the water to cement ratio, $i_{corr}(1)$ is the corrosion rate at the beginning of the corrosion propagation, and the cover is in mm. To calculate the corrosion rate after its initiation, another empirical formula that is presented in Eq. (9) can be used [16].

$$i_{corr}(t_p) = i_{corr}(1) \cdot 0.85t_p^{-0.29} \quad (9)$$

where t is the time at the starting stage of corrosion.

4.3. Reduction of the cross-sectional area of the sleeper bars

After the initial stage, the cross-section of the bars reduces due to the corrosion and this gradually imposes a negative impact on the sleeper strength. The decreasing sleeper strength leads to a decrease in the reliability index [13]. The equation for the determination of the reduction of the bars' cross-section can be written as follows [14]:

$$t \leq T_i \quad (10)$$

$$T_i < t < T_i + (D_i/2\lambda) \quad D(t) = \begin{cases} D_i \\ D_i - 2\lambda(t - T_i) \\ 0 \end{cases}$$

$$t > T_i + (D_i/2\lambda)$$

where t is the corrosion initiation time, λ is the corrosion rate at the surface, D is the initial bar diameter, and $D(t)$ is the changes in the bars diameter. The corrosion rate at the surface can be approximated as a function of i_{corr} . The resultant value of the corrosion is between [0.0116 and 0.116], which is about 32% of the maximum corrosion rate [12].

5. Time dependent analysis of the reliability

In the reliability analysis of the pre-stressed concrete sleepers, the maximum stress is considered to be present in either the rail seat or the mid-span, respectively. These are the areas of the sleeper where the maximum positive and negative bending moments exist [4]. To obtain the reliability index of the sleepers, the first step is to accurately define the limit state function as well as all the corresponding variables. Also, the statistical properties that influence the limit state function need to be determined.

5.1. Probabilistic model of the load and the strength

The concrete sleeper, due to its low water to cement ratio, has different statistical properties compared with the ordinary concretes. The main strength models of the concrete sleepers in this research are based on the characteristics and the experimental results that are obtained from the two main sleeper producing factories in Iran, during the years 2003–2007[6]. The lognormal distribution of the concrete strength is shown in Fig. 8. The Kolmogorov–Smirnov test indicates that the best distribution for the concrete strength among all other distributions is lognormal.



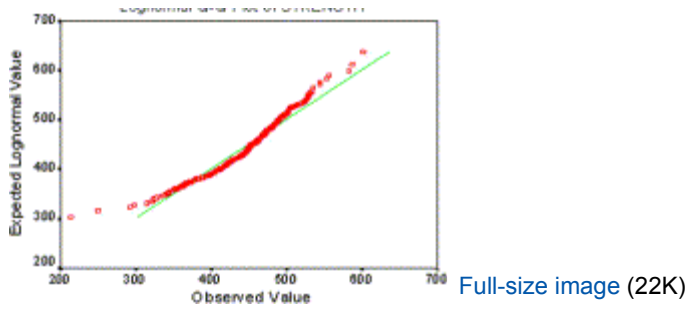


Fig. 8.

The Lognormal distribution of the concrete strength.

Table 3 presents the properties and the statistical models of the sleeper in the limit state function [17], [19] and [6].

Table 3. Statistical model of the selected PC sleeper.

Variable		Distribution type	average	Standard Deviation	coefficient of variation	Ref.
Width	$b(m)$	Normal	$b + 0.002$	0.003		[18]
Height	$h(m)$	Normal	$h + 0.002$	0.004		[18]
Axel load	P_d (KN)	Lognormal	125	21.25	0.17	[17]
Pre-stressing steel yield stress	f_{pe} (Mpa)	Normal	1100	44	0.04	[18]
Model coefficient	α	Normal	0.945	0.284	0.03	[18]
Dynamic intensification coefficient of bending moment	γ_i	Lognormal	1.6	0.48	0.3	[17]
Compression stress at transfer	f_{ci} (Mpa)	Lognormal	26.4	2.64	0.12	[6]
Tension stress at service	f_{te} (Mpa)	Lognormal	3.71	0.445	0.15	[6]
Compression stress at service	f_{ce} (Mpa)	Lognormal	24.75	2.475	0.12	[6]

5.2. The analysis of the reliability in operation

One method to obtain reliability of the pre-stressed concrete beams is the limit state function based on the allowable stress [18] and [19]. Equations of the limit state function in the analysis of the pre-stressed concrete reliability are listed hereunder. In these set of equations corrosion time function is not considered.

$$g_t(x) = \bar{\sigma}_t - \alpha \sigma_t$$

$$(11)$$

$$g_b(x) = \bar{\sigma}_b - \alpha\sigma_b \tag{12}$$

In the Eqs. (11) and (12) $\bar{\sigma}_t$ and $\bar{\sigma}_b$, are allowable stresses at the top and bottom fibers, respectively, and α is the variation coefficient of the model with respect to the sleeper resistance and the loading[18]. Due to the irregularities in the sleeper shape, concrete cover of the sleepers may have different thicknesses. Low concrete cover has direct impact on the time of the initial corrosion. Hence, the authors of this article use allowable stress method to calculate the variation of the sleeper reliability. Such method can help to investigate the variations in all points with tensile stress. Using the optimization toolbox of the Matlab software the reliability indices of the concrete sleeper are calculated at the rail seat and mid-span of the sleeper and are presented in Table 4[4].

Table 4. Reliability indices of B70 sleeper at rail seat and mid-span.

	Symbol	FORM	SORM	Monte Carlo
Reliability index at service in top fiber (mid-span)	β_{cte}	0.279	0.2620	0.2610
Reliability index at service in bottom fiber (mid-span)	β_{cbe}	0.9428	0.9424	0.9321
Reliability index at service in top fiber (rail seat)	β_{rte}	1.9468	1.9424	1.9321
Reliability index at service in bottom fiber (rail seat)	β_{rbe}	1.0854	1.8111	1.0431

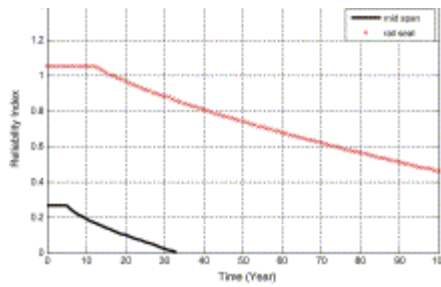
Considering the results in Table 4, it is indicated that the reliability index in tensile fiber is less than that in the compressive fiber. As a result, in order to clarify the sleeper failure time, investigation of the variations in the reliability with time is required.

5.3. Variation of the reliability with respect to time

In the sleeper time-dependent reliability analysis, it is assumed that the existing stresses in the sleeper are gradually increased while the allowable stress is constant. The limit state function also changes with the time. Assuming the time dependent stress variations, Eq. (11) can be rewritten as follows, [7].

$$g(x, t) = \bar{\sigma}_b - \alpha\sigma_b(t) \Rightarrow g(x, t) = R(t) - Q(t) \tag{13}$$

In Eq. (13) $g(x, t)$ is a time dependent limit state function and $\sigma_b(t)$ is the time dependent allowable stress in the bottom fiber; X is a variable of the limit state function and t is the time. Fig. 9 presents variation of the reliability at the top fiber of the mid-span and the bottom fiber of the rail seat.



[Full-size image \(38K\)](#)

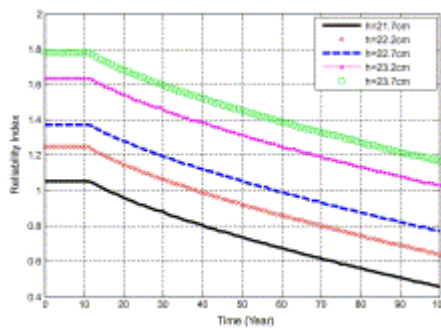
Fig. 9.

The reliability variations with time at the rail seat and mid-span.

According to Fig. 9, reliability of the mid-span top fiber reaches zero after 33 years, which indicates that the sleeper failure is probable by this time. Railway periodic maintenance reports also indicate that the sleeper replacement time is approximately about what is shown in Fig. 9[2].

5.4. The Sensitivity analysis of reliability variations

The difference between the sleeper sections at the rail seat and the mid-span is a decisive factor that can make the reliability indices of these sections, different. The reliability of the Pre-stressed concrete structures is more sensitive to dimension alternations compared with the ordinary concrete structures. Considering dimension variations, the sleeper, with the new dimension, is analysed once more by using the initial loading condition and the stresses in the new section are calculated. Fig. 10 and Fig. 11 show the reliability variations in the top and the bottom fiber versus dimension variations in the sleeper.



[Full-size image \(58K\)](#)

Fig. 10.

The effect of the height variation on the reliability indices of the B70 sleepers at the rail seat.

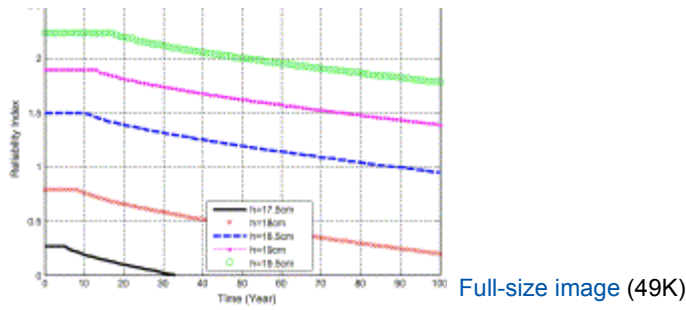


Fig. 11.

The effect of the height variation on the reliability indices of the B70 sleepers at the mid-span.

When the height of the sleeper section is increased, the concrete cover on the bars would increase accordingly. Based on Eq. (6), it is confirmed that the time of the corrosion initiation increases with the increase in the concrete cover. The corrosion rate and the reliability reduction rate would decrease, accordingly. For instance, the reliability reduction rate in the sleeper mid-span with the height of 19.5 cm is lower than that of 17.5 cm.

Considering the UIC713 code, the speed of travel and the axle load of the train are effective factors on the sleeper loading and the static rail forces [9]. UIC713 code recommends decreasing the axle load for the speed of travel over 200 km/h (a general issue to be noted for high speeds). The variation in the reliability, due to the different speeds and loadings of the trains, is shown in two cases in Fig 12 and Fig 13. In the 1st case, the axle load is constant and is equal to 18 tonnes while the train speed changes. In the 2nd case, the train speed of 180 km/h is constant while its' loading changes.

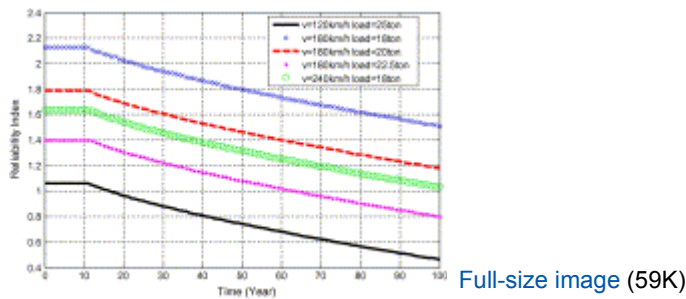
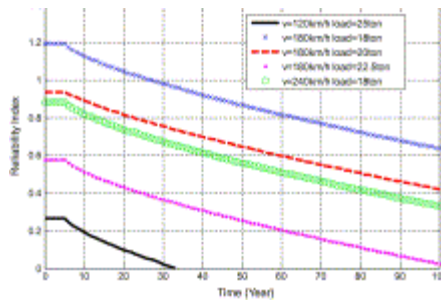


Fig. 12.

The effect of the axle load and speed variations on the reliability indices of the B70 sleepers at the mid-span.



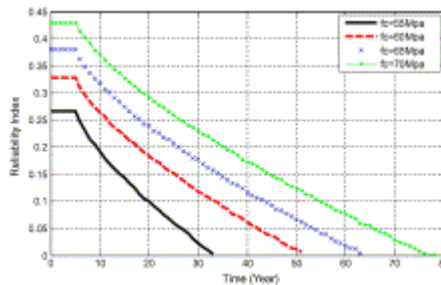
Full-size image (55K)

Fig. 13.

The effect of the axle load and speed variations on the reliability indices of the B70 sleepers at the rail seat.

It is clear from the results in Fig. 12 that decrease in the axle load while the speed of travel is kept constant, results in the increased reliability. For instance, if the train speed increases to more than 200 km/h (in constant axle load of 18 tonnes), the reliability index in the bottom fiber would then decrease from 2.16 to 1.62. This is an indicator of the fact that the reliability is sensitive to the speed variations according to the UIC713 code.

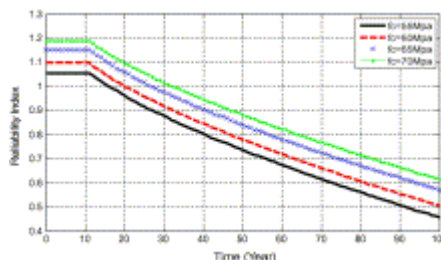
In railway sleeper analysis based on the allowable stress, there is a direct relationship between the concrete strength and the allowable stress. According to Eq. (12), increase in the concrete strength causes an increase in the bending strength and the reliability index. Fig. 14 and Fig. 15 illustrate the effect of the strength variation on the reliability indexes of the PC sleepers.



Full-size image (49K)

Fig. 14.

The effect of the concrete strength variation on the reliability indices of the B70 sleepers at the mid-span.



Full-size image (49K)

Fig. 15.

The effect of the concrete strength variation on the reliability indices of the B70 sleepers at the rail seat.

Due to the fact that the reliability index in the sleeper mid-span is less than that of the rail seat, it can be concluded that the mid-span is more sensitive to the concrete strength variations and the increase in concrete strengths causes higher increase in the reliability of the sleeper mid-span.

6. Conclusion


This article presented the results of an investigation into the reliability variations in the top fiber of the sleeper mid-span and the bottom fibers of the rail seat. As a result of the low reliability index in the top fiber of the sleeper mid-span combined with the low concrete cover in this part of the sleeper, it is concluded that the sleeper mid-span is more vulnerable than the rail seat.

Also comparing the increased amount of the concrete strength and the increased height of the sleeper section proves that the reliability variations in the sleeper mid-span are higher when the height is increased. Obviously, the cost of increasing the sleeper strength overrides the cost of increasing the height [4]. Therefore, the best choice to enhance the reliability index of the concrete sleeper is to increase its' height.

The rate of the reliability reduction with respect to the load, strength and cover variations has a similar, constant and descending process. This similarity is due to the constant environmental conditions.

References

- [1] Arnold D. Kerr, Fundamentals of railway track engineering, Simmons Boardman Publishers Co. (2003).
- [2] RAI, Iranian railway track frequently inspection report; 2002..
- [3] Philip S. Marsha and Dan M. Frangopol, Reinforced concrete bridge deck reliability model incorporating temporal and spatial variations of probabilistic corrosion rate sensor data. *Reliab Eng Syst Safety*, (2008), pp. 394–409.
- [4] Vahabi E, Evaluation of reliability indices of pre- stressed concrete sleepers, M.Sc. thesis, Iran University of Science and Technology; 2009..
- [5] Kaewunruen S, Remennikov A. Reliability assessment of railway Pre-stressed concrete sleepers. Australasian Structural Engineering Conference (ASEC); 2008..
- [6] Mohammadzadeh S. Iranian Railway research Centre, Experiments Results; 2003-2007 (in Persian)..
- [7] R.E. Melchers, Structural reliability analysis and prediction, Ellis Horwood Limited, Cambridge, UK (1987).
- [8] Manual for Railway Engineering – Chapter 30 – Ties” American Railway Engineering and Maintenance-of-Way Association; 2006..
- [9] EN 13230-2(2004): Railway application – Track. – Concrete sleepers and bearers – Part 2: Pre-stressed monoblock sleepers..
- [10] Naway EG. Pre-stressed concrete a fundamental approach. The McGraw-Hill -fourth edition; 2003..
- [11] Gjörv OE. durability design of concrete structures in severe environments. Taylor & Francis Journal, First published; 2009..

- [12] Stewart MG. Spatial variability of pitting corrosion and its influence on structural fragility and reliability of rc beams in flexure. *Struct Safety* 26(4): p. 453–70..
- [13] Duprat Fre´de´ric, Reliability of RC beams under chloride ingress. *Construct Build Mater*, **21** 8 (2007), pp. 1605–1616.
- [14] Stewart MG, Estes AC, Frangopol DM. Bridge deck replacement strategies and life-cycle cost analyses under multiple limit states. *Proc Int Conf on Bridge Safety*; 2002..
- [15] Jan Bijen, Durability of engineering structures: Design, repair and maintenance: CRC-First published; 2003..
- [16] K.A.T. Vu and M.G. Stewart, Structural reliability of concrete bridges including improved chloride-induced corrosion models. *Struct Safety*, **4** (2000), pp. 13–333.
- [17] Mohamadzadeh S. Reliability analysis of concrete railway bridges with slab and beam system, P.H.D thesis. Iran University of science and technology; 2000..
- [18] Al-Harthy. Reliability analysis and reliability-based design of pre-stressed concrete structures. PhD thesis. Department of Civil Engineering, University of Colorado atoulder, USA; 1992..
- [19] S. Barakat, N. Kallas and M.Q. Taha, Single objective reliability-based optimization of pre-stressed concrete beams. *Comput Struct*, (2003), pp. 2501–2512. [Article](#) |  [PDF \(481 K\)](#) | | [View Record in Scopus](#) | | [Cited By in Scopus \(4\)](#)



Corresponding author. Tel.: +98 9123184943.

Copyright © 2010 Elsevier Ltd. All rights reserved.

Engineering Failure Analysis

Volume 18, Issue 1, January 2011, Pages 421-432

[Home](#) [Browse](#) [Search](#) [My settings](#) [My alerts](#) [Shopping cart](#)

About ScienceDirect
[What is ScienceDirect](#)
[Content details](#)
[Set up](#)
[How to use](#)
[Subscriptions](#)
[Developers](#)

Contact and Support
[Contact and Support](#)

About Elsevier
[About Elsevier](#)
[About SciVerse](#)
[About SciVal](#)
[Terms and Conditions](#)
[Privacy policy](#)
[Information for advertisers](#)

Copyright © 2011 [Elsevier B.V.](#) All rights reserved. SciVerse® is a registered trademark of Elsevier Properties S.A., used under licen
 Elsevier B.V.